Lycorine (Lycoris radiata)- A unique natural medicine on breast cancer

Qinbing Xue
Engineering Research Center for Medicine, Ministry of Education, Harbin University of Commerce
Bing Wang
School of Food Engineering, Harbin University of Commerce
Jie Feng
Engineering Research Center for Medicine, Ministry of Education, Harbin University of Commerce
Chaoyu Li
Engineering Research Center for Medicine, Ministry of Education, Harbin University of Commerce
Miao Yu
Engineering Research Center for Medicine, Ministry of Education, Harbin University of Commerce
Yan Zhao
Fourth Affiliated Hospital of Harbin Medical University
Zheng Qi (18645039597@163.com)
Engineering Research Center for Medicine, Ministry of Education, Harbin University of Commerce

Research Article

Keywords: Lycorine, Human breast cancer, Cell cycle arrest, Mitosis, Microtubule

Posted Date: September 28th, 2023

DOI: https://doi.org/10.21203/rs.3.rs-3349001/v1

Abstract

Background: Breast cancer (BC) is one of the most common types of cancer among women worldwide. Lycorine (*Lycoris radiata*), a small molecule derived from the traditional Chinese herb *Amaryllidaceae* plants, has appeared potential effect on inhibiting the growth of cancer cells and inducing apoptosis in various types of cancer with minor side effects.

Methods: To discuss the therapeutic effects and molecular mechanisms of lycorine on BC established by lycorine-treated S180 tumor-bearing mice in vivo and MTT assay in vitro. The mitotic arrest and microtubule morphology was observed by flow cytometry and fluorescence microscopy. Furthermore, both the mitotic and microtubule assembly dynamics genes were performed by qPCR assays, and the protein expression associated with mitotic arrest was investigated by flow cytometry and western blot.

Results: Lycorine was demonstrated to reduce sarcoma growth of S180 tumor-bearing mice (50.6 % at 40 mg/kg·bw of lycorine) and inhibit the proliferation of MCF-7 cells in concentration-dependent manner. Likewise, lycorine appeared little effect on the thymus and spleen indexes. Moreover, lycorine induced M phase cell cycle arrest viainterfering with the mitotic apparatus regulated the expression of 20 genes and 15 proteins in cell cycle progression. Furthermore, this study confirmed that the potential effect of lycorine on BC might be mediated by cell cycle arrest in M phase for the first time.

Conclusion: These results would be the consequence of exploitation of lycorine as a potential drug for BC therapy, however further preclinical and clinical studies are still needed.

Introduction

Cancer is the leading causes of death worldwide, by 2040, the number of new cases is expected to 29.5 million and the number of cancer-related deaths up to 16.4 million per year. Among these, breast cancer (BC) has surpassed lung cancer as the most common cancer in women, according for 12.5% of all new annual cancer cases in 2022 [1]. Women at increased risk of BC have several options to reduce, including surgery, lifestyle options and medication. Still, the therapeutic strategies against BC are mainly relied on resection and chemotherapy, on the other hand, the clinic treatment owns high risk of adverse side effects [2].

Traditional Chinese medicine (TCM) has garnered more attention for its definite curative effect and low toxicity [3, 4]. TCM has a long history of application on BC targeted therapies with growing popularity as promote postoperative physical recovery, reduce surgical complication rate, diminish the risk of recurrence and metastasis, attenuate chemotherapy toxicity, and reverse drug resistance [5]. Lycorine is a bioactive phenanthridine alkaloid extracted from bulbs of *Lycoris radiata* (family *Amaryllidaceae*), which possess effects of anti-cancer, antibacterial, anti-inflammatory, enzyme inhibitory, and analgesic effects [6, 7]. Moreover, aberrancy in cell cycle progression is the key mechanism underlying tumorigenesis, thereby, anticancer therapeutic targets is mainly depended on the regulating cell cycle progression [8].

However, the mechanisms underlying the therapeutic effects of lycorine on BC via cell cycle arrest are still unclear.

To data, cell cycle progression is mainly focused on both replication of genomic DNA and its subsequent segregation, where occur in eukaryotic cells during distinct cell cycle phases. Most of cancer cells are confirmed to undergo uncontrolled cell cycle progression, thereby, cell cycle checkpoints need to be defective for a cell to become cancerous [9]. This appeared to be consistent with previous study indicated that cancer cells are compromised to arrest the cell cycle instead of undergoing uncontrolled cell division [10]. Obviously, cell cycle arrest is essential for cancer cell viability, in this perspective, the differences between DNA damage check point and replication stress checkpoint responses are essential in the context of cancer. Analogously, cancer cells strongly rely on functional mitotic checkpoints to prevent catastrophic chromosome mis-segregation [11]. Taken together, cell cycle arrest phase could represent as an “Achilles’ heel” of cancer, which are crucial for cell cycle control and new therapeutic opportunities revealing.

To our knowledge, few studies have focused on the therapeutic effects of lycorine on BC by cell cycle progression. Thus, this study aims to (1) evaluate the anti-carcinoma cells effect of lycorine in vivo; (2) compare the inhibiting effect of lycorine on MCF-7, HepG2, MDA-MB-231, A549 and SGC-7901 cells; (3) confirm the cell cycle arrest of lycorine on BC by morphological observation; (4) and explore the mechanisms in both the relative expression of genes and proteins. This should be the consequence of lycorine exploitation as a potential drug for BC therapy.

Materials and methods

Chemicals and reagents

Human breast cancer cell line MCF-7, human hepatoma cell line HepG2, human breast carcinoma cell line MDA-MB-231, human gastric carcinoma cell line SGC-7901 and non-small cell lung cancer cell line A549 were passaged and maintained by the Postdoctoral Research Workstation of Engineering Research Center for Medicine, Harbin University of Commerce (Harbin, China). The carcinoma cell lines were cryopreserved and passaged (less than 50 generations) in laboratory. The Short Tandem Repeat (STR) was checked on National Infrastructure of Cell Line Resource website (Fig. S1). Lycorine was purchased from Aladdin Biotechnology (molecular formula: $C_{16}H_{17}NO_4$; purity > 98%, China, Fig. S2). Cyclophosphamide (CTX) and vincristine (VCR) were obtained from Yuanye Biotechnology (Shanghai, China). Fetal bovine serum (FBS) was purchased from Corning Life Science (New Zealand). RPMI-1640 medium and Dulbecco’s Modified Eagle Medium (DMEM) were obtained from Gibco (USA). PageRuler Prest Protein Ladder was from Fermentas Biotechnology (USA). 3-(4,5-dimethylthiazol-2-yl)-2,5-diphenyltetrazolium bromide (MTT), Phenylmethanesulfonyl fluoride (PMSF), Western and Cell Lysis buffer IP, BCA Protein Assay Kit were obtained from Beyotime Biotechnology (Jiangsu, China). DAB Concentrated Kit were purchased from Zhong Shan-Golden Bridge Biological Technology (Beijing, China). The primary antibodies against CyclinB1, CDK1, P21, Aurora A, Aurora B, p-H3, PLK1, BRCA1, BUBR1,

STAT3, PAK1, CAMK4, PKA, ERK1/2, GAPDH and β-actin were purchased from Bioss Biotechnology (Beijing, China). Secondary antibodies included horseradish peroxidase (HRP) anti-mouse or anti-rabbit and FITC-labeled goat anti-mouse were purchased from Beyotime Biotechnology (Jiangsu, China). All reagents used in this study were of analytical grade and the detailed instruments and reagents were listed in Table S1 and Table S2.

Animals and design

A total of 60 Kunming mice (clean grad, half male and half female, 4 weeks old and weighing 20 ± 2 g) were bought from Liaoning Changsheng Biotechnology Co. Ltd. (experimental animal license: SCXK (Liao) 2010-0001), and maintained in a temperature-controlled room with 12 h light/dark cycle and free access to food and water given. All experimental procedures were conducted according to the guide for the affidavit of animal ethics and welfare allowed by the Animal Care and Use Committee of the Harbin University of Commerce (Fig. S3). S180 tumor cell was purchased from China Center for Type Culture Collection. Following a one-week adaption period, and the S180 cell line (2×10^6 cells/mL) was subcutaneous injection into the right flank of mice, when the diameters of tumors reached 1 cm after 7 days, mice were randomly divided into six groups (n = 10, half male and half female in each group): control, model (saline), lycorine low dose (10 mg/kg·bw), lycorine middle dose (20 mg/kg·bw), lycorine high dose (40 mg/kg·bw) and CTX (2 mg/kg·bw), and all groups were administered strictly once daily for 7 days in a volume of 0.2 mL, intraperitoneal injection. The S180 tumor-bearing mice were euthanized 24 h after the last administration. The tumors, thymuses and spleens were removed and weighed to calculate tumor weight, thymus index and spleen index. The tumor growth inhibition rate (IR) was calculated by the formula IR (%) = (1- TWt/TWm) × 100%, where TWt is the mean value of tumor weight after lycorine and CTX treatment, and TWm is the mean value of tumor weight of model group [12], spleen or thymus index (mg/g) = the weight of spleen or thymus (mg) / body weight (g).

Cell viability assay

MCF-7, HepG2, SGC-7901, A549 and MDA-MB-231 cells were cultured in 96-well plates with 10% fetal bovine serum and various concentrations of lycorine (2, 4, 8, 16, 32 and 64 μmol/L) for 24 h (n = 6). Then, 50 μL of 0.5 mg/mL MTT solution was added to each well and incubated at 37°C in a humidified incubator with 5% CO_2 for 4 h. After incubation, the supernatant was discarded and 150 μL of DMSO was added into each well. Finally, the absorbance values (OD values) of cells were read at 490 nm using a microplate reader for cell viability measurements.

Immunofluorescent and cell cycle progression detection

MCF-7 cells were treated with lycorine (7, 14 and 28 μmol/L) for 48 h, and VCR (0.625 μmol/L) was used as positive control intervention. The cells were washed three times with PBS solution, afterwards, the cells were stored in 75% ethanol at -20 ℃ overnight. Then, the fixed MCF-7 cells were stained in cold PI solution in the dark for 30 min. The OD values were read by a flow cytometer at an excitation wavelength of 488 nm, furthermore, the flow cytometric data were obtained using the Beckman-Coulter EPICS XL-MCL flow cytometer.

4% paraformaldehyde was used to fix MCF-7 α-tubulin cells in 6-well culture plates for 10 min. After that, cells were membrane permeabilized in 0.1% Triton X-100 for 5 min. In addition, 5% BSA blocking buffer was used to block the cells. Overnight at 4°C, cells were treated with a primary antibody against tubulin (1:1000). Then, the cells were washed in PBS solution twice. The sections were then treated with anti-goat IgG secondary antibody (1:3000) for 1.5 h. Finally, fluorescence microscope was then used to observe tubulin FITC stained MCF-7 cells.

Total RNA extraction and gene expression analysis

A total of cell cycle related 101 target genes of were detected and the primer sets were listed in Table S4. Among them, 13 microtubule-related gene (*ICIS, AURKB, CDC2, PAK1, STAT3, ERK, PKA, CAMK4, KIF2C, STMN1, KATNA1, MAP2* and *MAPT)* and 7 M-phase related gene (*CCNB2, CCNF, CDC25C, CDC6, CDC20, MRE11A* and *RAD51*) with high expression change were selected, which quantified in duplicate using Step One Plus™ Real-Time PCR system (Wcgene Biotech, Inc., Shanghai, China). The specificity of the qPCR products was also verified by melting curve analysis in Fig.S4, and the relative abundance of cycle arrest genes was calculated on the basis of $2^{-\Delta Ct}$ method, where $\Delta C_t = C_t$ (target gene)-C_t (internal reference gene).

Protein expression detection

The protein bands (CyclinB1, CDK1, p21, Aurora A, Aurora B, STAT3, PAK1, CAMK4, PKA, ERK1/2) were quantified by Image-pro plus 6.0 imaged using hypersensitive luminescence solution and the densitometry analysis. Subsequently, after FITC staining, 400-mesh nylon net was used to filter the cells. The relative fluorescence intensity of FITC-stained protein (p-H3, PLK1, BRCA1 and BUBR1) detected with flow cytometry was analyzed.

Statistical analysis

All experiments were repeated at least three times. Statistical analyses were performed using SPSS 15.0 statistical software, and the data were presented as mean ± standard deviation (SD). The Dunnett and Tukey test were performed to comparison between the treatment groups and control groups. Heatmap (Java Treeview 1.1.6) and Cluster 3.0 were used to analyze the correlation between proteins and genes expression, and $P < 0.05$ was considered statistical difference, $P < 0.01$ presented significant difference, and $P < 0.001$ presented extremely significant difference.

Results

Effects of lycorine on tumor weight, spleen index and thymus index in vivo

The schedule of animal experiment in vivo and cell assay in vitro was presented in Fig. 1. Lycorine dramatically suppressed tumor growth of S180 tumor-bearing mice and appeared a dose-dependent manner, the tumor inhibition rates were 21.7% (10 mg/kg·bw of lycorine), 32.1% (20 mg/kg·bw of

lycorine), 50.6% (40 mg/kg·bw of lycorine), respectively (Fig. 2A and Table S5). The tumor weight intervened by 40 mg/kg·bw lycorine (0.57 ± 0.13 g) were significantly reduced compared with the model group ($P < 0.001$), and its curative effect of high dose is consistent with that of CTX (0.49 ± 0.08 g). Following treatment with lycorine, the thymus and spleen indexes of S180 tumor-bearing mice appeared little effect (Fig. 2B, C), while there was no significant difference between high dose and low dose groups ($P = 0.079$, $P = 0.1470$, respectively). Additionally, the thymus and spleen indexes showed a significant decreased in CTX groups (0.88 ± 0.65, 3.11 ± 0.13, respectively) in comparison to high dose groups of lycorine (1.093 ± 0.28, 4.01 ± 0.53, respectively). These results indicated that lycorine could inhibit the immune function of S180 model mice as well as anti-tumor effect. Taken together, the aforementioned date indicated that lycorine could inhibit the growth of tumor, however lycorine appeared more therapeutic action on improving the tumor immunosuppressive microenvironment in S180 tumor- bearing mice.

Figure 1

Inhibition of lycorine on MCF-7, HepG2, MDA-MB-231, A549 and SGC-7901 cells in vitro

The inhibition rate of lycorine in dose of 64 μmol/L on cell viability in vitro was ranked as human breast cancer cell line MCF-7 (64.1%) > human hepatoma cell HepG2 (39.3%) > human breast carcinoma cell line MDA-MB-231 (34.4%) > human gastric carcinoma cell line SGC-7901(26.3%) and non-small cell lung cancer cell line A549 (26.3%) (Fig. 2D). The half-maximal inhibitory concentration (IC_{50}) values of lycorine on MCF-7 cells were 13.98 μmol/L (Table S3). In this way, three different doses (7, 14, 28 μmol/L) of lycorine were selected for the further experiments [13]. These results suggested that lycorine was revealed to capable of BC treatment in comparison to the other cancer cells.

Figure 2

Identification and analysis of cell cycle arrest

To validate whether lycorine could inhibit cell proliferation by the effect of inducing cell cycle arrest, the percentage of the cell cycle phases of MCF-7 cells was analyzed after treatment with lycorine. Lycorine induced the accumulation of cells in G2/M-phase cell-cycle arrest in a dose-dependent manner (Fig. 3A). The cells proportion of G2/M phase increased with the doses of lycorine from 11.14% (7 μmol/L), 15.47% (14 μmol/L) to 21.15% (28 μmol/L), which appeared significantly increased compared with the control group (9.53%), however it observed a gap curative effect between 28 μmol/L of lycorine and that of VCR (44.67%). Additionally, proportion of G0/G1 and S phase cells were considered no significant difference. The results demonstrated lycorine induced MCF-7 cell cycle arrest in G2/M phase arrest.

To investigate the cellular response to lycorine treatment induced G2/M phase cell cycle arrest, the morphological changes of MCF-7 cells was observed by immunofluorescence analysis (Fig. 3B, C). The results revealed that MCF-7 cells in control group had clear edges and regular shapes, α-tubulin was evenly distributed over the edges of the cells. In the VCR-treated group, cell fuzzy edges were observed

and cell volumes expanded in the MCF-7 cells. Moreover, after treating MCF-7 cells with lycorine for 48 h, the polymerization state of tubulin was altered, the distribution of morphology was disordered, the cells exhibited blurred edges, amplify in size, irregular shape and bent α-tubulin. Likewise, the high dose of lycorine (28 μmol/L) treatment groups showed a similar morphological changes of VCR treatment. Thus, these findings demonstrated that lycorine induced tubulin polymerization at the cellular and molecular levels, which indicated that lycorine had tubulin-targeting function in MCF-7 cells.

Figure 3

Abundance expression of cell cycle-regulatory genes

To elucidate the underlying mechanisms, the cell cycle-regulatory genes were examined by qPCR assay. Genetic changes are the primary signal of cellular changes, in this way, all the genes of 101 in cell cycle were detected, among them, a sub of 9 genes (*AURKB, CDC2, PAK1, STAT3, ERK, PKA, CAMK4, MAP2 and MAPT*) down regulated and 4 genes up regulated (*ICIS*, *KIF2C, STMN1* and *KATNA1*) in microtubule (Fig. 4A), a sub of 7 genes (*CCNB2, CCNF, CDC25C, CDC6, CDC20, MRE11A and RAD51*) down regulated in M-phase (Fig. 4B). The effect of lycorine on MCF-7 by regulating the expression of intracellular cycle-related genes was performed in order to further capture the interactions between 20 genes (Fig. 4C). These 20 related genes were divided into four categories, the relative abundance expression of *MRE11A, STAT3, PAK1, PKA, AURKB, CCNB2* and *CDC25C* were similar, genes *CDC6, MAP2, CDC20, CCNF, MAPT* and *RAD51* clustered in one category, the expression of *CAMK4, ERK* and *CDC2* were similar, while *KATNA1, ICIS, STMN1* and *KIF2C* were clustered in one category. The results suggested that the down-regulation of *STAT3 CAMK4 PKA PAK1 ERK ICIS Aurkb and CDC2* may be involved in the accumulation of genes *STMN1*and *KIF2C* in lycorine treated MCF-7 cells. On the other hand, the expression of genes in control group and low dose of lycorine presented similar, and high dose of lycorine was revealed same effect with VCR group.

Figure 4

Cell cycle arrest-related protein expression

To further confirm the effect of lycorine on cell cycle arrest-related protein activity, a total of 15 protein expression was discussed both in microtubule and M-phase (Fig. S5, Table. S8). Specifically, western blot analysis revealed that lycorine enhanced the expression of microtubule associated marker p21, but decreased the expression of CyclinB1, CDK1, Aurora A, Aurora B, STAT3, CAMK4, PAK1, PKA, ERK1 and ERK2 in MCF-7 cells after 48 h (Fig. 5.A, B, G). Furthermore, lycorine also significantly upregulated the expression of mitotic phase marker p-H3 and BUBR1 (Fig. 5.C, F) and down-regulated the expression of PLK1 (Fig. 5.D), however the expression of BRCA1 had no obvious variation (Fig. 5.E). The results indicated that lycorine triggered the M-phase cell cycle arrest in MCF-7 cells.

To further determine the potential role of proteins in cell cycle arrest, principal component analysis (PCA) was performed. Among the cycle arrest relative proteins, PLK1, STAT3, PAK1, CAMK4 and PKA were clustered in PC1, which explained 88.8% of the first component. p21 and BUBR1 accounted for 6.4% in

PC2, while the other presented 3.1% in PC3 (Fig. 5H and Table S6). The cell cycle arrest in MCF-7 cell induced by lycorine was revealed, at least partly, due to alterations in the expression of cell cycle-related proteins. Moreover, these findings suggested that lycorine-induced M-phase cell cycle arrest may mediated by PLK1, STAT3, PAK1, CAMK4 and PKA.

Figure 5

Mechanism of lycorine inhibiting effect on breast cancer

To test the therapeutic effects of lycorine on mitotic arrest in MCF-7 cells, cluster analysis and correlation analysis were performed on 20 related genes of 15 proteins. The darker color indicated higher expression of genes and proteins, and the thicker lines presented the stronger related between genes and proteins (Fig. 5A and Table S7). Protein CDK1 and gene *STMN1, KIF2C, KATNA1, STAT3, ERK*, protein CyclinB1 and gene *STMN1, KATNA1*, protein p21 and gene *STMN1, KIF2C, KATNA1*, protein Aurora A and gene *KATNA1*, protein Aurora B and gene *KATNA1*, protein ERK and gene *KATNA1* in the MCF-7 cells were extremely significant correlated ($P < 0.01$).

By contrast, the cell cycle progression was classified into 2 types, which were M phase (80%), and G2 phase (20%). The results indicated that lycorine induced cell cycle arrest mainly in M phase. Meanwhile, the expression of M phase-related protein ranked as STAT3 (15.62%) > PAK1 (13.09%) > CAMK4 (12.55%) > PKA (9.65%) > PLK1 (7.72%) > BRCA1 (7.26%) > BUBR1 (6.59%) > p-H3 (5.92%) > ERK2 (5.33%) > ERK1 (5.30%), followed by Aurora B of 4.87%. Cyclin B1, p21 and CDK1 accounted for the fraction of 44.68%, 28.19% and 27.13% in G2 phase, respectively (Fig. 5B). All these results indicated that lycorine significant inhibited MCF-7 cell cycle arrest in M phase.

Figure 6

Discussion

BC remains a recalcitrant cancer in women worldwide, thus novel therapeutic strategies of TCM with low side effects are urgently needed. Lycorine, the active alkaloid isolated from *Lycoris radiata* (family *Amaryllidaceae*) has a long history of application in TCM [14, 15], and has been reported to possess extensive pharmacological activities, such as anti-inflammatory, antiviral, and antitumor effects [16]. Previous studies reported that lycorine not only has inhibitory effects on tumor growth but also has extensive activity that induces apoptosis [14]. As mentioned earlier, lycorine suppressed constitutive STAT3 activation by up-regulating the expression of SHP-1 and down-regulating the expression of STAT3 target proteins, thus induced apoptosis and cell cycle arrest. However, more research is needed to fully understand potential therapeutic effect of lycorine as a drug of BC treatment and its safety profile. In the present study, we found that lycorine had inhibiting effect on BC both in vivo and in vitro for the first time.

Immunosuppression appears to be a major side effect of chemotherapy drugs, while it is not disturbing for lycorine. Instead, the lycorine suppressed tumor growth based on their altered immunostimulatory activities. Thymus and spleen are the important immune organs, which orchestrate adaptive immune

responses [17]. CTX was the most effective drug evaluated against 33 kinds of cancers out of 1,000 anti-tumors compounds and medicines [18], however, it accompanied by high toxicity and severe side effects. Thus, it was worth noting that lycorine suppressed tumor growth in addition to lessening the frequency of the aforementioned adverse effects.

By contrast, stomach cancer, lung cancer and liver cancer and BC are the top four cancers with high morbidity and mortality [19–21]. Moreover, the inhibitory effects of lycorine on the growth of MCF-7, MDA-MB-231, SGC-7901, A549 and HepG-2 cells were demonstrated by MTT assay in vitro. Studied to identify the active alkaloids with anti-proliferative activities and the corresponding sensitive cell lines, lycorine had obvious inhibitory effects on MCF-7 cell proliferation in a dose-dependent manner, and the IC_{50} values of lycorine for MCF-7 cells was 13.98 μmol/L. Last but not least, the MCF-7 cells were considered sensitive to lycorine.

Cell cycle arrest is a process by which the normal progression of the cell cycle is disrupted. This can occur in response to various signals, such as DNA damage, replication stress, and oncogene activation [22]. It has been proposed as a therapeutic strategy for the treatment of cancer [23]. However, the mechanism that lycorine induces cell cycle arrest is still unclear. Firstly, the results demonstrated lycorine induced MCF-7 cell cycle arrest in G2/M phase arrest by flow cytometer. Furthermore, a sub of 101 genes in cell cycle were detected, among them, 20 target genes and 15 cell cycle arrest related proteins with high expression changes were discussed. More importantly, CDK1 and CyclinB1 are critical in G2 phase checkpoint. CyclinB1 progressively increases through G1 and S phase and reaches its peak in G2 phase then form complex with CDK1. It has been documented that CDK1 is activated on centrosomes, CyclinB1-CDK1 binds to the microtubules, chromosomes and to unattached kinetochores in the prometaphase [24]. Recent literature reports that evodiamine induced M-phase cell cycle arrest via the p21 signaling pathway in ESCC cells [25]. In our study, the expression of protein p21 was up-regulated by lycorine treatment. The expression of protein CDK1 was down-regulated by p21, which caused the down regulation CyclinB1 further inhibited the activity of CDK1 in MCF-7 cells. The Phosphorylation of Histone H3 (p-H3) is a critical step in the regulation of the cell cycle, playing a key role in the regulation of DNA replication and chromosome segregation [26]. During the cell cycle, p-H3 modification occurs in the early stages of mitosis and marks the chromatin for proper condensation and separation. CyclinB1 and Histone H3 phosphorylation are the markers of cells in M phase. Our experiment revealed that lycorine treatment significantly enhanced the mitotic phase marker protein p-H3 expression, indicating that lycorine triggered the M-phase cell-cycle arrest in MCF-7 cells, instead of the G2 phase. These findings suggested that lycorine induced M-phase arrest may be mediated by p21.

The phosphorylation of p-H3 is catalyzed by mitotic kinases, such as Aurora A and Aurora B, which recognize and bind to the p-H3 modified histones. Any disruptions in p-H3 phosphorylation levels may lead to a variety of chromosomal abnormalities and contribute to the development of diseases such as cancer [27]. Herein, the down-regulated expressions of protein Aurora A and Aurora B induced by lycorine in this study revealed in this study. Likewise, PLK1 was the key checkpoint to recovery from mitotic arrest mediated by the DNA damage after DNA damage repair [28]. BUBR1 is a very important protein in mitotic

checkpoint, which plays a role in maintaining checkpoint activation in chromosome kinetochore and cytoplasm, and its expression peaks at G2/M phase with the progress of cell cycle. Aurora-B is involved in the enrichment and phosphorylation of BUBR1. When the lack of appropriate tension is detected at the mitotic spindle detection point, it can effectively prevent the continuation of mitosis. Meanwhile, BUBR1 can be phosphorylated by PLKl. In the present study, we demonstrated that lycorine-induced down-regulated expression in PLK1 and up-regulated expression in BUBR1. Taken together, induction of mitotic arrest in MCF-7 cells was occurred.

Apart from cell-cycle arrest, triggering microtubules dynamics is another appealing option for cancer treatment. The relationship between microtubules and cancer is complex and multifaceted. In cancer cells, alterations in microtubule dynamics can result in changes to cell division and lead to the formation of abnormal, uncontrolled growths [29]. The microtubule targeting agents (MTAs) used in cancer chemotherapy work by disrupting the normal structure and stability of microtubules, leading to cell cycle arrest and apoptosis. Here, we investigated for the first time whether lycorine hampers the mitotic effect through the inhibition of microtubule dynamics in MCF-7 cells. Oncoprotein stathmin 1 (STMN1), also known as oncoprotein 18, is involved in the regulation of the microtubule 561 dynamics system. Accumulating evidence shows that STMN1is highly expressed in multiple 562 types of human cancer, which functions as a tumor promoter contributing to malignant phenotypes [30]. Mitotic centromere-associated kinesin (MCAK/KIF2C) is a member of the kinesin-13 family, which is important for the regulation of microtubule dynamics. Moreover, disrupting the dynamic balance of microtubule depolymerization and polymerization is a potential target for the development and research of antitumor drugs [13]. In a nutshell, the results in this study proved that lycorine down-regulated expression of pro-microtubule polymerization related genes (*MAP2, MAPT*), and up-regulated the expression of microtubule depolymerization-related genes (*STMN1, KIF2C, KATNA1*) in MCF-7 cells.

Conclusions

In summary, this study uncovered a mechanism by lycorine induced BC through regulating cell-cycle arrest. Activation of p21/CDK1/CyclinB1 signaling pathway involved in underlying mitotic cell cycle arrest in MCF-7 cells was validated. Obviously, lycorine disrupted tubulin morphology and the dynamic balance of tubulin polymerization and depolymerization. These findings demonstrated for the first time that the inhibitory activity of lycorine in MCF-7 cells, by which led to M-phase cell cycle arrest, DNA damage and enhance microtubule dynamics.

Furthermore, these results imply that lycorine has the great prospect in the clinical treatment of BC and also has great significance for enriching the application of TCM in the development of new anti-tumor drugs. Notably, TCM focuses on the characteristics of multi-target and multi-mechanism treatment of diseases, and thus the potential effect of lycorine on BC might be mediated by cell cycle arrest in M phase via targeting multiple tumorigenic pathways. Further studies will carry out the potential molecular mechanism of therapeutic action of lycorine on BC by microRNAs, long non-coding RNAs and circular

RNAs. Last but not least, our findings would be the consequence of exploitation of lycorine as a potential drug for BC therapy, however further preclinical and clinical studies are still needed.

Abbreviations

BC, breast cancer; CTX, cyclophosphamide; DMEM, RPMI-1640 medium and Dulbecco's Modified Eagle Medium; FBS, fetal bovine serum; MTT, 3-(4,5-dimethylthiazol-2-yl)-2,5-iphenyltetrazolium bromide; PMSF, phenylmethanesulfonyl fluoride; STR, the short tandem repeat; TCM, traditional Chinese medicine; VCR, vincristine;

Declarations

Funding Declaration

This study was supported by the National Natural Science Foundation of China (Grant No.: 41702368), the Outstanding Young Talents Project of the Central Government's Reform and Development Fund for Local Universities (Grant No.: 2020YQ12), and the Key Research and Development Program of Heilongjiang Province (Grant No.: 2022ZX02C07).

Ethics Statement

All animal experiments in this study were approved by the Harbin University of Commerce Animal Care and Use Committee (HSDYXY-20210020). Informed consent was obtained from each participant. Extensive efforts have been made by researchers to ensure that the animals used in the study suffer minimally.

Consent for publication

Not applicable.

Date Availability Statement

The datasets generated and/or analyzed during the current study are available from the corresponding author on reasonable request.

CRediT authorship contribution statement

QBX and JF: Conceptualization, Methodology, Software, Writing-original draft. BW, YZ, and CYL: Data detection, Software. MY: Conceptualization, Supervision, Funding acquisition. ZQ: Conceptualization, Writing-review & editing, Supervision.

Conflict of interests

All authors declare no potential conflicts of interest.

References

1. H. Sung, J. Ferlay, R. L. Siegel, M. Laversanne, I. Soerjomataram, A. Jemal, F. Bray, Global cancer statistics 2020: GLOBOCAN estimates of incidence and mortality worldwide for 36 cancers in 185 countries, CA-Cancer. J. Clin. 71 (2021) 209–249, https://doi.org/10.3322/caac.21660.
2. K. L. Britt, J. Cuzick, K. A. Phillips, Key steps for effective breast cancer prevention, Nat. Rev. Cancer. 20 (2020) 417–436. https://doi.org/10.1038/s41568-020-0266-x.
3. Y. Xie, C. T. Mai, D. C. Zheng, Y. F. He, S. L. Feng, Y. Z. Li, C. X. Liu, H. Zhou, L. Liu, Wutou Decoction Ameliorates Experimental Rheumatoid Arthritis via Regulating NF-KB and Nrf2: Integrating Efficacy-Oriented Compatibility of Traditional Chinese Medicine, Phytomedicine. 85 (2021) 153522. https://doi.org/10.1016/j.phymed.2021.153522.
4. L. Bu, O. Dai, F. Zhou, F. Liu, J. F. Chen, C. Peng, L. Xiong, Traditional Chinese medicine formulas, extracts, and compounds promote angiogenesis, Biomed. Pharmacother. 132 (2020) 110855. https://doi.org/10.1016/j.biopha.2020.110855.
5. Z. M. Yang, Q. H. Zhang, L. H. Yu, J. Y. Zhu, Y. Cao, X. F. Gao, The signaling pathways and targets of traditional Chinese medicine and natural medicine in triple-negative breast cancer, J. Ethnopharmacol. 264 (2021) 113249. https://doi.org/10.1016/j.jep.2020.113249.
6. A. G. Atanasov, S. B. Zotchev, V. M. Dirsch, the International Natural Product Sciences Taskforce, C. T. Supuran, Natural products in drug discovery: advances and opportunities, Nat. Rev. Drug. Discov. 20 (2021) 200–216. https://doi.org/10.1038/s41573-020-00114-z.
7. S. S. Yin, S. S. Yang, Y. M. Luo, J. Lu, G. Y. Hu, K. L. Wang, Y. Y. Shao, S. Y. Zhou, S. Koo, Y. L. Qiu, T. Wang, H. Y. Yu, Cyclin-dependent kinase 1 as a potential target for lycorine against hepatocellular carcinoma, Biochem Pharmacol. 193 (2021) 114806. https://doi.org/10.1016/j.bcp.2021.114806.
8. J. Liu, Y. H. Peng, W. Y. Wei, Cell cycle on the crossroad of tumorigenesis and cancer therapy, Trends Cell Biol. 32 (2021) 30–44. https://doi.org/10.1016/j.tcb.2021.07.001.
9. N. Molinie, S. N. Rubtsova, A. Fokin, S. P. Visweshwaran, N. Rocques, A. Polesskaya, A. Schnitzler, S. Vacher, E. V. Denisov, L. A. Tashireva, V. M. Perelmuter, N. V. Cherdyntseva, I. Bièche, A. M. Gautreau, Cortical branched actin determines cell cycle progression, Cell. Res. 29 (2019) 432–445. https://doi.org/10.1038/s41422-019-0160-9.
10. H. K. Matthews, C. Bertoli, R. A. M. Bruin, Cell cycle control in cancer, Nat. Rev. Mol. Cell. Bio. 23 (2022) 74–88. https://doi.org/10.1038/s41580-021-00404-3.
11. G. J. P. L. Kops, D. R. Foltz, D. W. Cleveland, Lethality to human cancer cells through massive chromosome loss by inhibition of the mitotic checkpoint, P. Natl. Acad. Sci. USA. 101 (2004) 8699–8704. https://doi.org/10.1073/pnas.0401142101.
12. J. L. Guo, Q. L. Wang, Y. Zhang, W. H. Sun, S. Z. Zhang, Y. C. Li, J. Y. Wang, Y. M. Bao, Functional daidzein enhances the anticancer effect of topotecan and reverses BCRP-mediated drug resistance

in breast cancer, Pharmacol. Res. 147 (2019) 104387. https://doi.org/10.1016/j.phrs.2019.104387.

13. L. Yu, S. Han, L. Lang, H. Song, C. Y. Zhang, L. Dong, S. H. Jia, Y. Zhang, D. Xiao, J. Liu, Y. Xu, X. P. Zhang, Oxocrebanine: a novel dual topoisomerase inhibitor, suppressed the proliferation of breast cancer cells MCF-7 by Inducing DNA Damage and Mitotic Arrest, Phytomedicine. 84 (2021) 153504. https://doi.org/10.1016/j.phymed.2021.153504.
14. H. X. Xiao, X. Z. Xu, L. Y. Du, X. Y. Li, H. D. Zhao, Z. Wang, L. Zhao, Z. Yang, S. F. Zhang, Y. Yang, C. Y. Wang, Lycorine and organ protection: review of its potential effects and molecular mechanisms, Phytomedicine, 104 (2022) 154266. https://doi.org/10.1016/j.phymed.2022.154266.
15. F. N. Li, Q. Y. Zhang, O. Li, S. L. Liu, Z. Y. Yang, L. J. Pan, C. Zhao, W. Gong, Y. J. Shu, P. Dong, ESRRA promotes gastric cancer development by regulating the CDC25C/CDK1/CyclinB1 pathway via DSN1, Int. J. Biol. Sci. 17 (2021) 1909–1924. https://doi.org/10.7150/ijbs.57623.
16. Y. H. Jin, J. S. Min, S. Jeon, J. Lee, S. Kim, T. Park, D. Park, M. S. Jang, C. M. Park, J. H. Song, H. R. Kim, S. Kwon, Lycorine, a non-nucleoside RNA dependent RNA polymerase inhibitor, as potential treatment for emerging coronavirus infections, Phytomedicine. 86 (2021) 153440. https://doi.org/10.1016/j.phymed.2020.153440.
17. J. F. Miller, A scientific odyssey: uncovering the secrets of thymus function, Cell. 179 (2019) 21–26. https://doi.org/10.1016/j.cell.2019.08.023.
18. A. Emadi, R. J. Jones, R. A. Brodsky, Cyclophosphamide and cancer: golden anniversary, Nat Rev Clin Oncol. 6 (2009) 638–647. https://doi.org/10.1038/nrclinonc.2009.146.
19. C. E. Weeden, W. Hill, E. L. Lim, E. Grönroos, C. Swanton, Impact of risk factors on early cancer evolution, Cell. 186 (2023), 1541–1563. https://doi.org/10.1016/j.cell.2023.03.013.
20. E. Nolan, G. J. Lindeman, J. E. Visvader, Deciphering breast cancer: from biology to the clinic, Cell. 186 (2023) 1708–1728. https://doi.org/10.1016/j.cell.2023.01.040.
21. W. Zhou, M. Dong, H. Wu, H. L. Li, J. L. Xie, R. Y. Ma, W. W. Su, J. Y. Dai, Common mechanism of Citrus Grandis Exocarpium in treatment of chronic obstructive pulmonary disease and lung cancer, Chin. Herb. Med.13 (2021) 525–533. https://doi.org/10.1016/j.chmed.2021.08.005.
22. P. Icard, L. Fournel, Z. R. Wu, M. Alifano, H. Lincet, Interconnection between metabolism and cell cycle in cancer, Trends Biochem SCI. 44 (2019) 490–501. https://doi.org/10.1016/j.tibs.2018.12.007.
23. J. M. Suski, M. Braun, V. Strmiska, P. Sicinski, Targeting cell-cycle machinery in cancer, Cancer. Cell. 39 (2021) 759–778. https://doi.org/10.1016/j.ccell.2021.03.010.
24. F. N. Li, Q. Y. Zhang, O. Li, S. L. Liu, Z. Y. Yang, L. J. Pan, C. Zhao, W. Gong, Y. J. Shu, P. Dong, ESRRA promotes gastric cancer development by regulating the CDC25C/CDK1/CyclinB1 pathway via DSN1, Int J Biol Sci. 17 (2021) 1909–1924. https://doi.org/10.7150/ijbs.57623.
25. L. Zhang, L. H. Li, X. H. Chen, S. Y. Yuan, T. Xu, W. L. Zhao, M. Li, F. Y. Wang, R. M. Hoffman, L. J. Jia, Evodiamine inhibits ESCC by inducing M-phase cell-cycle arrest via CUL4A/p53/p21 axis and activating noxa-dependent intrinsic and DR4-dependent extrinsic apoptosis, Phytomedicine. 108 (2023) 154493. https://doi.org/10.1016/j.phymed.2022.154493.

26. B. B. Ren, E. S.Chen, Regulation of centromeric heterochromatin in the cell cycle by phosphorylation of histone H3 tyrosine 41, Curr. Genet. 65 (2019) 829–836. https://doi.org/10.1007/s00294-019-00962-2.
27. C. Y. Zhang, Y. J. Guan, J. N. Zou, X. Yang, G. Bayliss, S. G. Zhuang, Histone methyltransferase MLL1 drives renal tubular cell apoptosis by p53-dependent repression of E-cadherin during cisplatin-induced acute kidney injury, Cell. Death. Dis. 13 (2022) 770. https://doi.org/10.1038/s41419-022-05104-0.
28. C. A. Raab, M. Raab, S. Becker, K. Strebhardt, Non-mitotic functions of polo-like kinases in cancer cells, BBA-Rev. Cancer. 1875 (2021) 188467. https://doi.org/10.1016/j.bbcan.2020.188467.
29. R. Zheng, Y. L. Du, X. T. Wang, T. L. Liao, Z. Zhang, N. Wang, X. M. Li, Y. Shen, L. Shi, J. H. Luo, J. Xia, Z. Y. Wang, J. Y. Xu, KIF2C regulates synaptic plasticity and cognition in mice through dynamic microtubule depolymerization, Elife. 11 (2022) 72483. https://doi.org/10.7554/elife.72483.
30. L. Liao, Y. L. Zhang, L. Deng, C. Chen, X. Y. Ma, L. Andriani, S. Y. Yang, S. Y. Hu, F. L. Zhang, Z. M. Shao, D. Q. Li, Protein phosphatase 1 subunit PPP1R14B stabilizes STMN1 to promote progression and paclitaxel resistance in triple-negative breast cancer, Cancer. Res. 83 (2023) 471–484. https://doi.org/10.1158/0008-5472.can-22-2709.

Figures

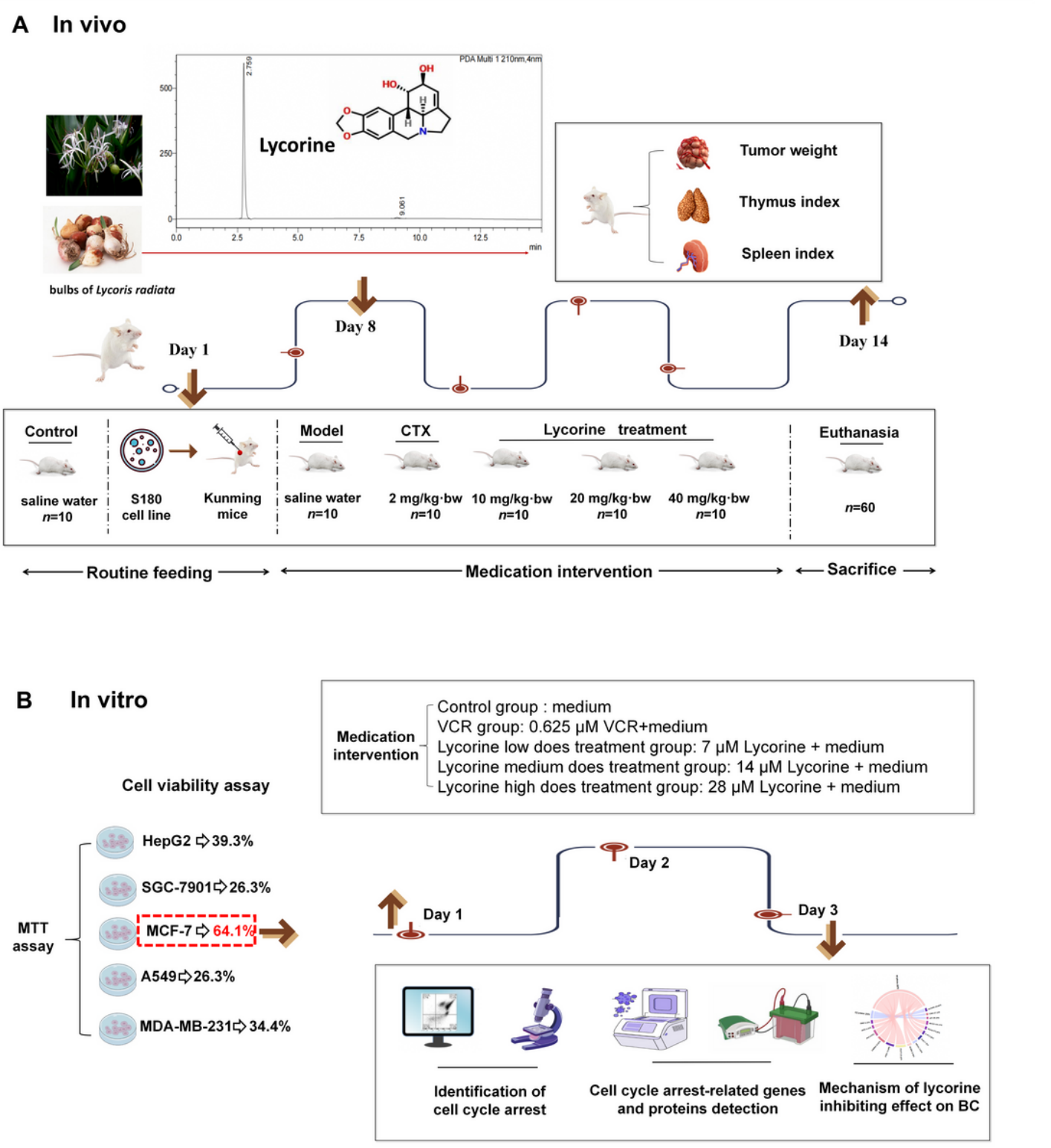

Figure 1

The schedule of experimental design. (A) Study design of animal experiment and treatment in vivo. (B) Study design of cell experiment in vitro.

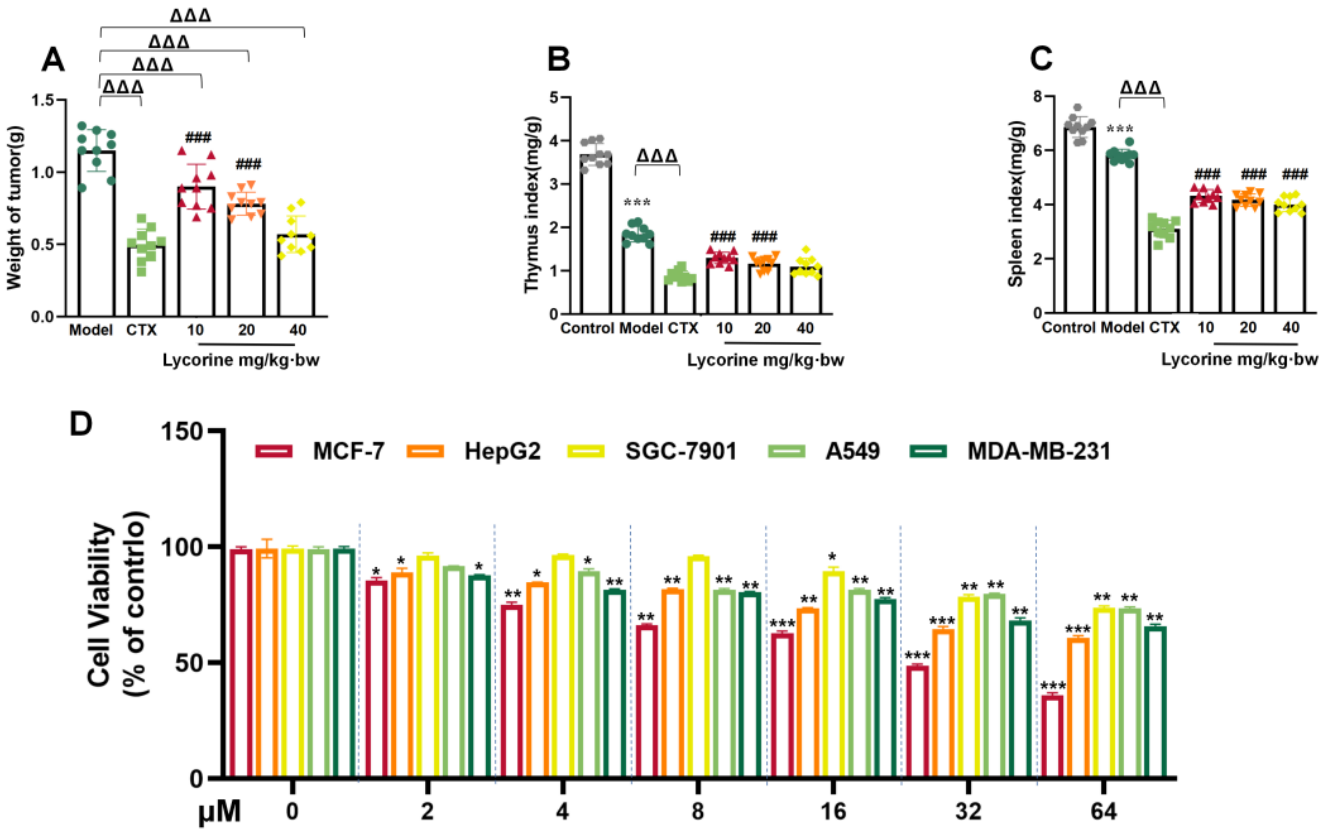

Figure 2

Lycorine inhibited S180 tumor growth and stimulated the host immune response. (A) Tumor weights of mice in each group (*n*=10). (B) Thymus indexes of mice in each group (*n*=10). (C) Spleen indexes of mice in each group (*n*=10). (D) The cell viability variation of MCF-7, HepG2, SGC-7901, A549 and MDA-MB-231 cells treated with lycorine of 2, 4, 8, 16, 32 and 64 μmol/L (*n*=6). Data were expressed as mean±standard deviation. Significant difference was indicated as $^{\#\#\#}P < 0.001$ presented extremely significant difference compared with the CTX group. * $P < 0.05$, ** $P < 0.01$ and *** $P < 0.001$, compared with the control group. $^{***}P < 0.001$, compared with the model group. $^{\Delta\Delta\Delta}P < 0.001$, compared with the model group.

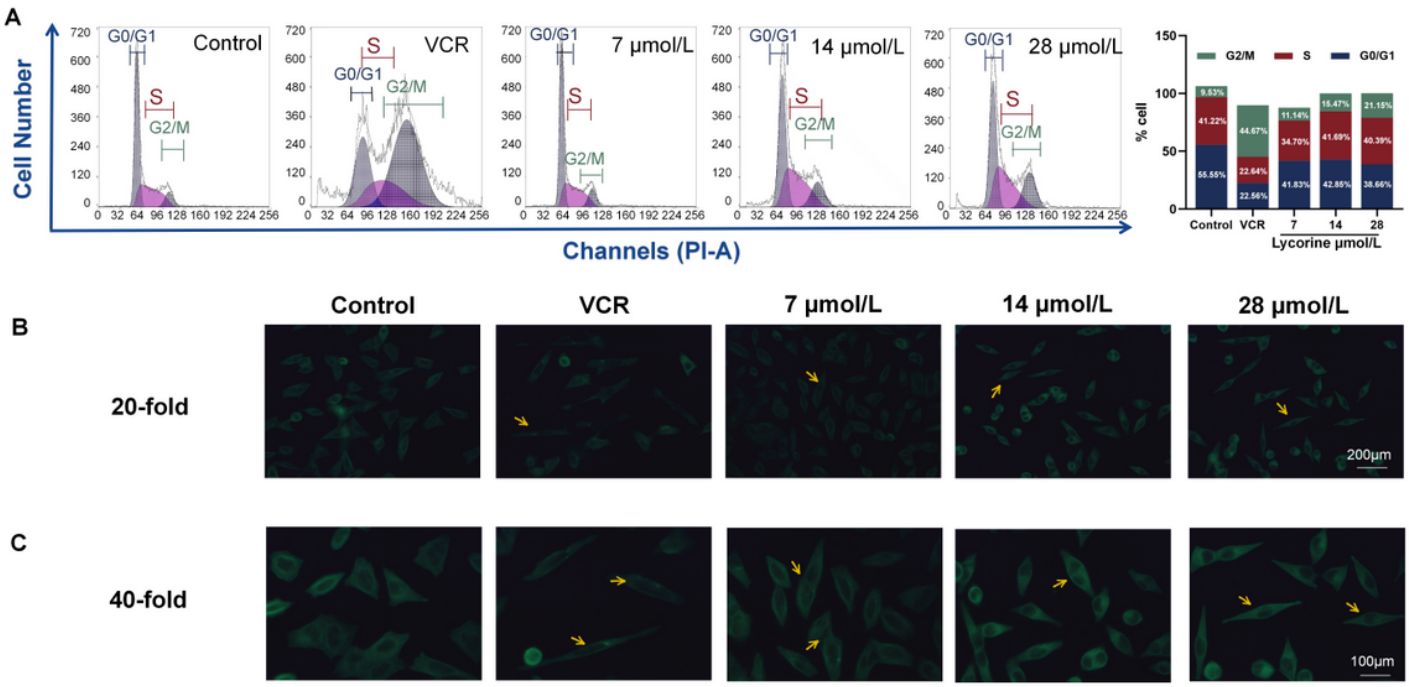

Figure 3

Lycorine induced cell cycle arrest in MCF-7 cells. (A) Flow cytometric analysis of phases percentage of the cell cycle in MCF-7 cells treated with lycorine (7 μmol/L, 14 μmol/L, 28 μmol/L), 0.625 μmol/L VCR for 24 h and stained with PI. (B) × 20, (C) ×40 α-tubulin changes detected by fluorescence microscopy. Anti α-tubulin and FITC-conjugated goat anti-rabbit IgG (green) were used to label microtubules. Yellow arrows presented abnormal α-tubulin morphology in MCF-7 cells.

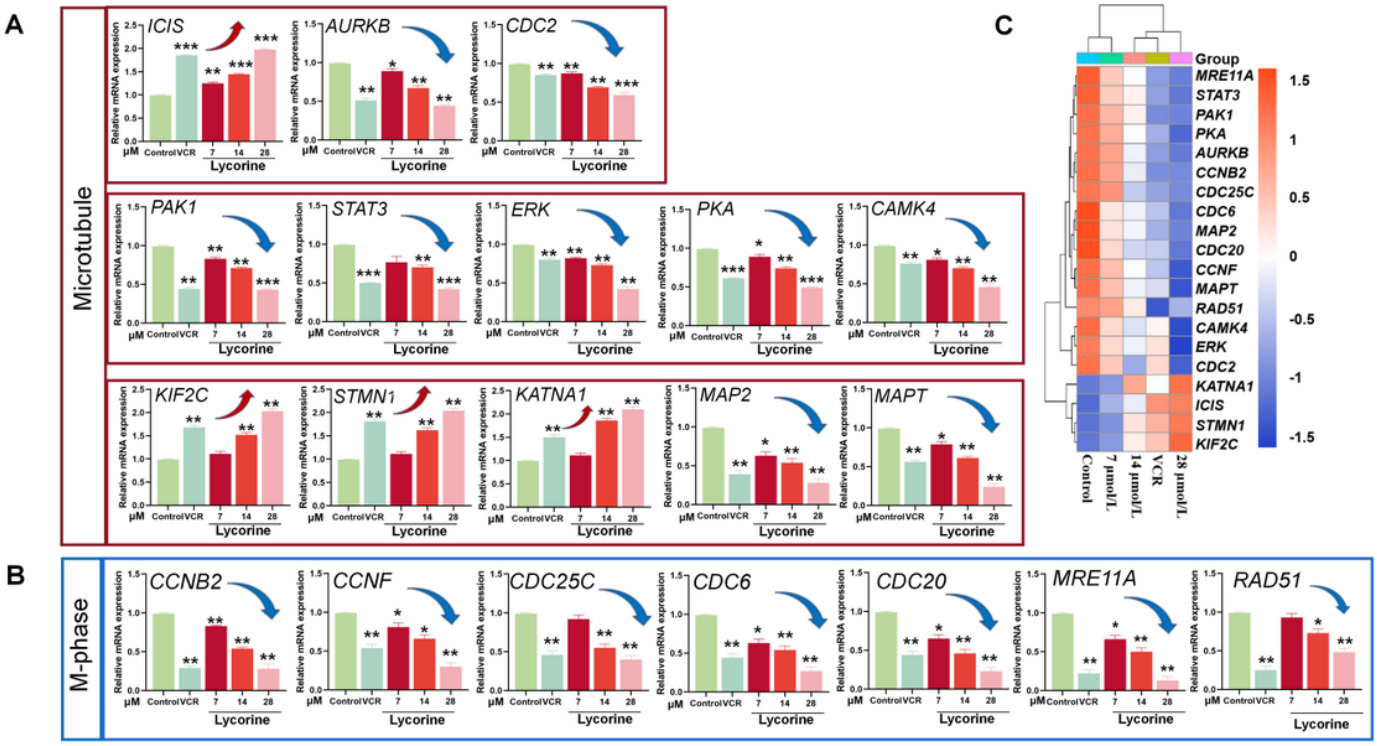

Figure 4

Effect of lycorine treatment on expression of relative genes in MCF-7 cells. (A) Effect of lycorine on the expression of microtubule relative genes in MCF-7 cells (*n*=3). (B) Effect of lycorine on the expression of M-phase relative genes in MCF-7 cells (*n*=3). (C) Heatmap of various doses of lycorine treatment on MCF-7 intracellular cycle-related gene expression. Significant differences indicated as **P* < 0.05, ***P* < 0.01 and ****P* < 0.001 compared with the control group.

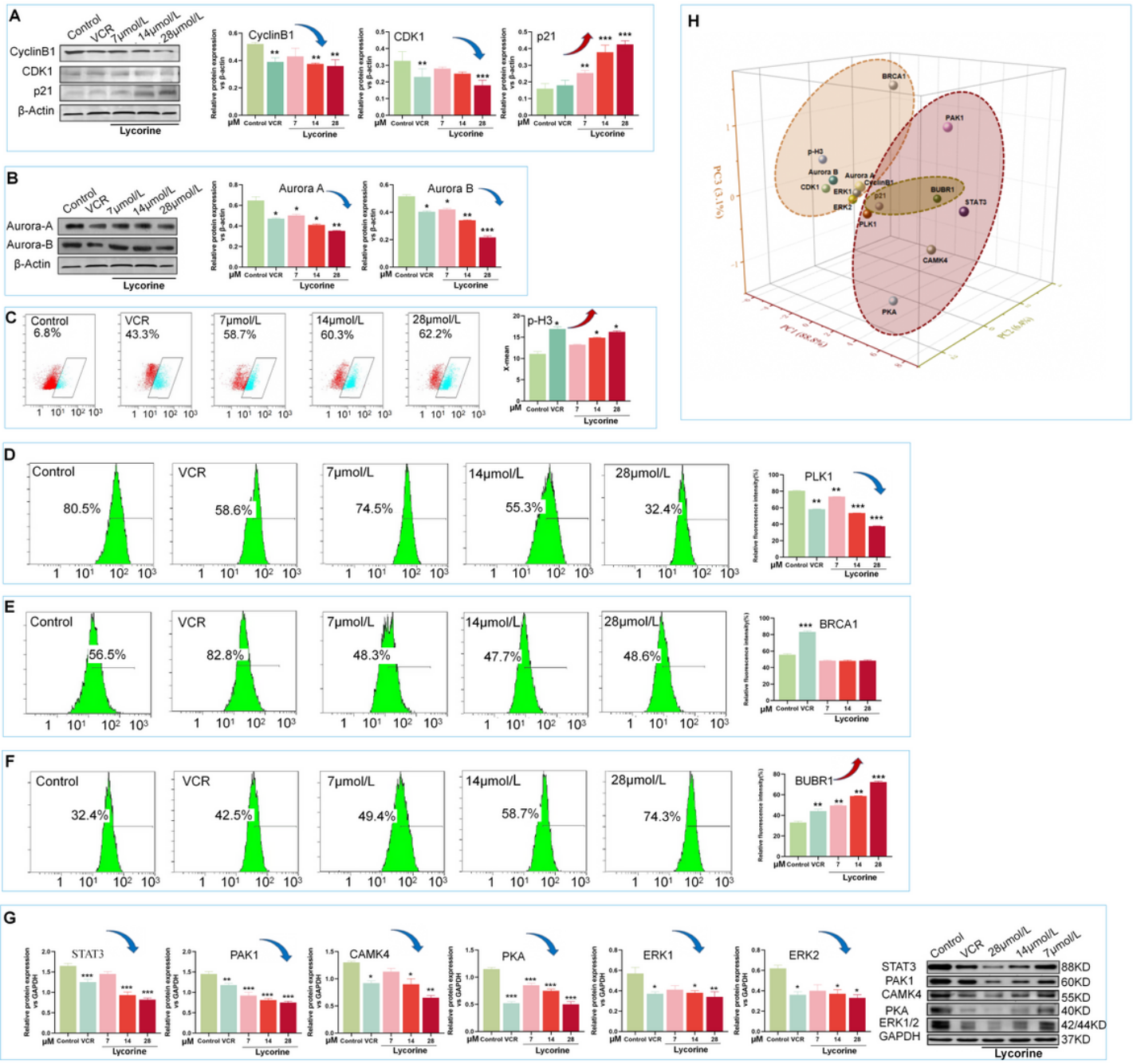

Figure 5

Expression of proteins in cell cycle arrest. (A) Expression of protein CyclinB1, CDK1, p21 by western blot. (B) Expression of protein Aurora A and Aurora B by western blot. (C, D, E, F) Quantification of the p-H3, PLK1, BRCA1 and BUBR1 protein in cells by FITC staining with flow cytometry. (G)Expression of protein STAT3, PAK1, CAMK4, PKA and ERK by western blot. (H) PCA ordination plot for eigenvalue decomposition covariance matrixes among cell cycle arrest relative proteins based on the relative abundance. Significant differences were indicated as $*P < 0.05$, $**P < 0.01$ and $***P < 0.001$ compared with the control group.

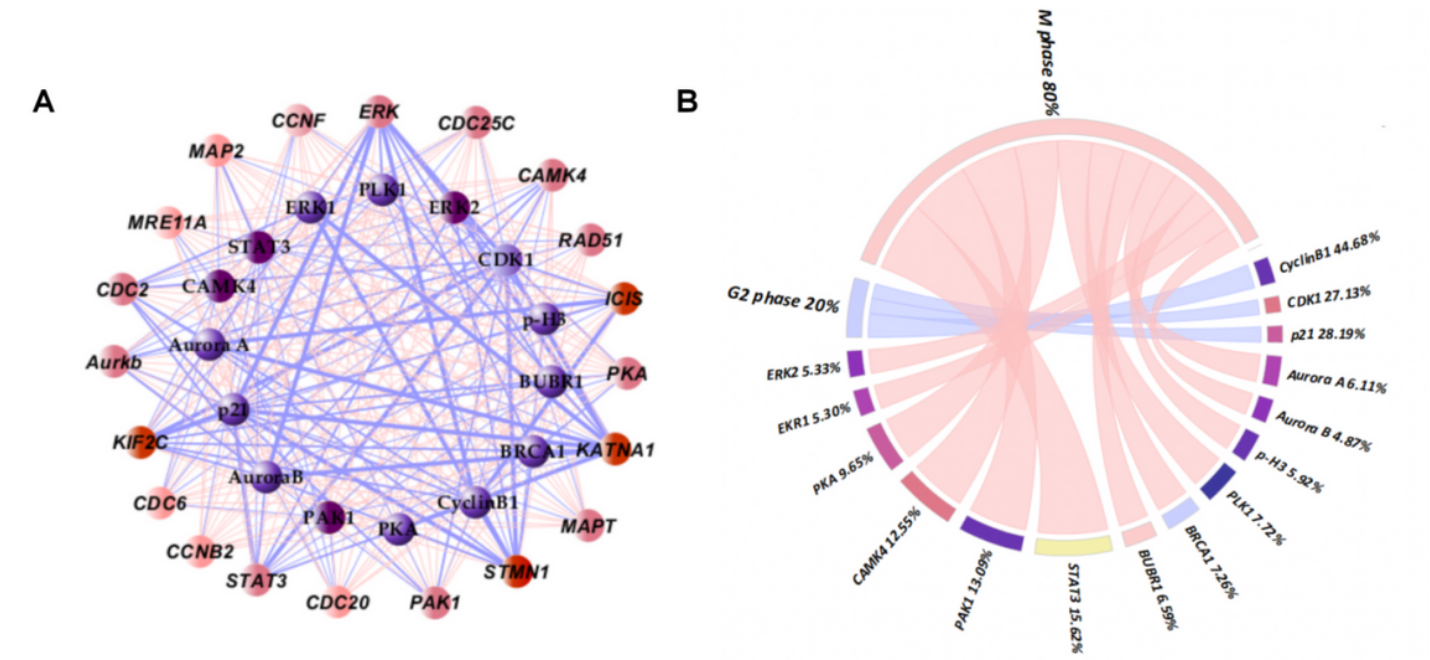

Figure 6

The mechanism of lycorine-induced cell cycle arrest related. (A) Correlation between cell cycle arrest related proteins and genes. (n = 3, the darker color indicated the greater contribution in proteins and genes, and the thicker line indicated more statistical significance (P < 0.01). (B) The contribution of proteins analyzed by chord diagram. The size of the connected ribbon indicated by the shared cell cycle and proteins.

Supplementary Files

This is a list of supplementary files associated with this preprint. Click to download.

- SupplementaryMaterials.docx